Short Article

Cell Host & Microbe

The Oxidative Stress Network of *Mycobacterium tuberculosis* Reveals Coordination between Radical Detoxification Systems

Graphical Abstract

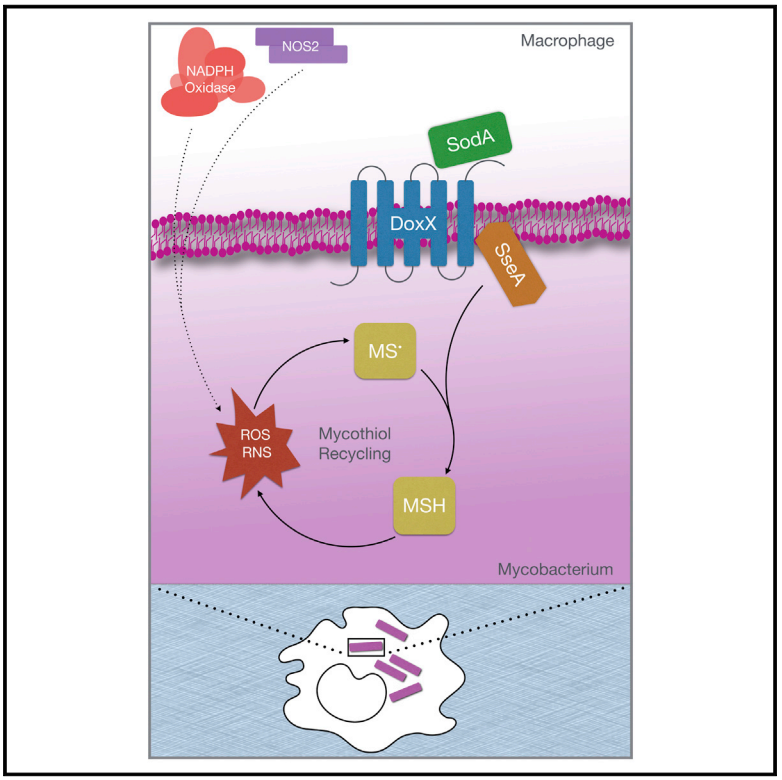

Authors

Subhalaxmi Nambi, Jarukit E. Long, Bibhuti B. Mishra, ..., Hien P. Nguyen, Scott A. Shaffer, Christopher M. Sassetti

Correspondence

christopher.sassetti@umassmed.edu

In Brief

Host-derived oxidants impose stress on *Mtb* and limit its growth. How *Mtb* coordinates resistance to oxidative stress remains unclear. Nambi et al. define the *Mtb* oxidative stress network during infection and identify the membrane-associated oxidoreductase complex, a three-protein complex that coordinates ROS detoxification with thiol homeostasis as required for infection.

Highlights

- In vivo *Mtb* screen identifies the membrane-associated oxidoreductase complex (MRC)
- The MRC coordinates ROS detoxification and thiol homeostasis during infection
- Loss of the MRC reduces thiol recycling and increases sensitivity to oxidative damage
- *Mtb* mutants of MRC components are highly attenuated

Nambi et al., 2015, Cell Host & Microbe *17*, 829–837
June 10, 2015
http://dx.doi.org/10.1016/j.chom.2015.05.008

Cell Host & Microbe
Short Article

The Oxidative Stress Network of *Mycobacterium tuberculosis* Reveals Coordination between Radical Detoxification Systems

Subhalaxmi Nambi,[1] Jarukit E. Long,[1] Bibhuti B. Mishra,[1] Richard Baker,[1] Kenan C. Murphy,[1] Andrew J. Olive,[1] Hien P. Nguyen,[3] Scott A. Shaffer,[3] and Christopher M. Sassetti[1,2,*]
[1]Department of Microbiology and Physiological Systems, University of Massachusetts Medical School, 55 Lake Avenue N., Worcester, MA 01655, USA
[2]Howard Hughes Medical Institute, 4000 Jones Bridge Road, Chevy Chase, MD 20815, USA
[3]Proteomics and Mass Spectrometry Facility and Department of Biochemistry and Molecular Pharmacology, University of Massachusetts Medical School, 55 Lake Avenue N., Worcester, MA 01655 USA
*Correspondence: christopher.sassetti@umassmed.edu
http://dx.doi.org/10.1016/j.chom.2015.05.008

SUMMARY

***M. tuberculosis* (*Mtb*) survives a hostile environment within the host that is shaped in part by oxidative stress. The mechanisms used by *Mtb* to resist these stresses remain ill-defined because the complex combination of oxidants generated by host immunity is difficult to accurately recapitulate in vitro. We performed a genome-wide genetic interaction screen to comprehensively delineate oxidative stress resistance pathways necessary for *Mtb* to resist oxidation during infection. Our analysis predicted functional relationships between the superoxide-detoxifying enzyme (SodA), an integral membrane protein (DoxX), and a predicted thiol-oxidoreductase (SseA). Consistent with that, SodA, DoxX, and SseA form a membrane-associated oxidoreductase complex (MRC) that physically links radical detoxification with cytosolic thiol homeostasis. Loss of any MRC component correlated with defective recycling of mycothiol and accumulation of cellular oxidative damage. This previously uncharacterized coordination between oxygen radical detoxification and thiol homeostasis is required to overcome the oxidative environment *Mtb* encounters in the host.**

INTRODUCTION

A cornerstone of metazoan immunity is the production of anti-microbial oxygen and nitrogen radicals by phagocytes. In mammals, superoxide (O_2^-) is generated by the phagocyte NADPH oxidase and xanthine oxidase systems (Halliwell and Gutteridge, 2007). While this reactive species can interact directly with its targets, the superoxide radical is also converted into a number of chemically distinct oxidants, such as peroxide (H_2O_2), hypochlorite (HClO), hydroxyl radicals (OH·), and peroxynitrite ($ONOO^-$). Together, these species damage microbial DNA, lipids, and proteins, as well as particularly susceptible cellular constituents such as iron-sulfur (4Fe-4S) cluster proteins.

The complexity of the phagocyte oxidative burst is matched by the numerous strategies used by bacterial pathogens, such as *M. tuberculosis* (*Mtb*), to resist these insults. Virtually all cells protect themselves from oxidative stress using a cytosolic thiol redox buffer, such as the tripeptide, glutathione. In *Mtb*, the functional analog of glutathione is the cysteine glycoconjugate, mycothiol (Newton et al., 1996). In addition to this common redox buffering system, *Mtb* stress defense mechanisms also include dedicated antioxidant enzymes such as superoxide dismutase (SOD), catalase/peroxidase (KatG), thioredoxin reductase (Tpx), alkylhydroperoxide reductase (AhpC), and peroxiredoxin (AhpE) (Bryk et al., 2002; Edwards et al., 2001; Jaeger et al., 2004; Wilson and Collins, 1996).

Despite the identification of several enzymes that could protect *Mtb* from defined oxidative stresses, it remains unclear how the activities of these pathways are coordinated. Genetic interaction (GI) studies have the capacity to systematically define functional relationships between genes or pathways. A GI is defined by two mutations that modify the phenotype of the other. Aggravating interactions often result from loss-of-function mutations in redundant genes that produce a greater than additive effect. Alleviating interactions occur between genes in the same pathway that depend upon one another for their function and therefore produce a less than additive effect when simultaneously mutated. In order to understand the functional network that *Mtb* employs to resist the oxidative stresses produced during infection, we delineated a comprehensive GI network centered on SOD activity.

RESULTS

Delineating the Oxidative Stress Network during Infection

The primary oxidant produced by the phagocyte oxidative burst is superoxide. Defining a comprehensive oxidative stress interaction network required an *Mtb* mutant that is sensitive to this radical, as well as the array of additional superoxide-derived oxidants produced in vivo. The major SOD of *Mtb*, SodA, is essential for bacterial viability, and therefore not useful for this GI

study. However, the P-type ATPase (CtpC) responsible for metalating SodA with Mn^{2+} is known, and cells lacking *ctpC* are both viable and sensitive to superoxide (Padilla-Benavides et al., 2013). We leveraged this SodA hypomorph to generate a global GI map of oxidative stress resistance during infection in mice.

Saturated transposon libraries were generated in wild-type (WT) *Mtb* and the *ctpC::hyg* background. As described previously (Sassetti and Rubin, 2003; Joshi et al., 2006) both libraries were subjected to a period of selection in the mouse spleen, an environment in which the bacteria encounter the full complexity of host-derived oxidants. Surviving mutants were recovered from these animals, and the relative representation of each transposon mutant was compared between the WT and *ctpC::hyg* libraries to generate a map of 181 aggravating or alleviating mutations (Figures 1A–1C). This number of interacting genes was consistent with that observed for highly connected "hub" genes in *S. cerevisiae* and *E. coli* GI maps, and our previous GI studies in *Mtb* (Babu et al., 2014; Costanzo et al., 2010; Griffin et al., 2011; Joshi et al., 2006). Among the previously recognized ROS detoxification systems, the peroxiredoxin, *ahpE*, showed the strongest interaction with *ctpC* (Table S1), whereas weaker and statistically non-significant interactions were found with *katG* and *ahpCD*. In addition, a much more complex network emerged that was composed of several distinct functional classes of genes, discussed below (Figure 1C).

Alleviating interactions were detected between *ctpC* and iron homeostatic genes, such as those in operons involved in siderophore synthesis (*mbtA-N*), the *irtAB*-encoded siderophore importer (Chavadi et al., 2011; Farhana et al., 2008), an iron-sulfur cluster assembly protein (*rv1465*), and the ferric uptake regulation protein (*furA*). This is consistent with the known role of Fe^{2+} in potentiating oxidative stress via the Fenton reactions (Winterbourn, 1995) and suggests that cytosolic ferric iron concentration is a significant determinant of oxidative damage during infection.

Several other interacting pathways indicate a major role for redox cofactor homeostasis in oxidative stress resistance in vivo. The reduction of both nicotinamide- (NAD^+) and flavin-derived (F420) cofactors via succinate dehydrogenase (*rv0247c-rv0249c*) and the F420-dependent glucose dehydrogenase (*fgd*) (Hasan et al., 2010) were found to promote oxidative stress resistance. Mutations in central carbon metabolism and respiration produced both alleviating and aggravating effects, which are also likely related to the maintenance of the redox state of cofactors.

The aggravating effect of mutations in genes necessary for the synthesis or modification of the major outer membrane lipids, phthiocerol dimycocerosate and mycolic acid, could also be related to $NADP^+$/NADPH homeostasis as mycobacteria regulate lipid anabolism as a mechanism of redox control (Singh et al., 2009). However, genes involved in subtle chemical modifications of mycolates, such as methylation (*mmaA1*) or cyclopropanation (*mmaA2*), also potentiated oxidative damage, suggesting a distinct role for the cell envelope in resistance. The observed function for ESX (type VII) secretion systems in cell envelope biogenesis (Garces et al., 2010) may similarly explain the presence of these genes in the network.

Finally, mutations in cysteine synthetic and catabolic genes had opposing effects on oxidative stress resistance. Blocking cysteine synthesis via mutation of *cysM* aggravated the *ctpC* phenotype. Conversely, inhibition of cysteine catabolism to alanine via mutation of *iscS* alleviated this phenotype. These complementary GIs suggested that the availability of cysteine, or small-molecular-weight thiols derived from cysteine, might be a critical determinant of oxidative stress resistance during infection. In sum, the architecture of the *Mtb* oxidative stress network affords a quantitative assessment of the cellular functions that are important for resisting the complex mixture of oxidants encountered during infection, and illustrates functional interactions between the canonical oxidative defense mechanism imparted by SOD activity and a variety of other cellular functions including thiol metabolism (Tables S1 and S2; Figure 1C).

SodA Exists in a Membrane-Associated Thiol Oxidoreductase Complex

To understand the biochemical basis for the identified GI, we used a mass spectrometry-based approach to determine if members of the GI network formed stable protein complexes. When a FLAG-tagged allele of Rv3005c, one of the strong alleviating interactors of *ctpC*, was purified from detergent extracts of *Mtb*, two additional proteins were co-purified (Figures 2A and S1). One was SseA (Rv3283), another strong alleviating interactor of *ctpC.* The second was SodA, which depends on CtpC for its metalation. This complex of functionally related proteins was evolutionarily conserved, as we found that these three proteins also co-purified from lysates of *M. smegmatis* (*Msm*), a saprophytic relative of *Mtb* (Figure 2B). In addition to this conserved complex, a small number of additional Rv3005c-interacting partners were found in *Mtb*, which function in either sulfur metabolism or oxidative defense (Figure 2A).

Homology indicated that the two SodA-interacting proteins of *Mtb* could be involved in sulfur redox reactions. The hypothetical protein, Rv3005c, is predicted to contain 4–5 transmembrane domains and is weakly homologous to "Dox" proteins of chemotrophic archea that contribute to sulfur oxidation (Müller et al., 2004). SseA is predicted to be a member of a ubiquitous family of thiosulfate sulfurtransferases (TSTs) that are most commonly thought to alleviate cyanide toxicity by converting cyanide to thiocyanate (Cipollone et al., 2007). However, TST-like enzymes play diverse roles, and can also act as thiol oxidoreductases (Nandi et al., 2000). In particular, their ability to regenerate glutathione thiyl radicals has been proposed to explain the oxidative stress sensitivity of *A. vinelandii* TST mutants (Remelli et al., 2012). The possible roles for Rv3005c and SseA in thiol redox reactions, and their physical and GIs with SodA, led us to hypothesize that this three-protein complex might coordinate multiple enzymatic functions necessary for oxidative stress resistance during *Mtb* infection. Henceforth, we will refer to Rv3005c as "DoxX."

To directly investigate if DoxX and SseA possess biochemical functions consistent with oxidative stress resistance, we examined the thiosulfate oxidizing activity of the complex using potassium ferricyanide as an electron acceptor. We generated mutant strains of both *Msm* and *Mtb* lacking SseA (*ΔMsmeg_1809*, *Δrv3283*) or DoxX (*ΔMsmeg_2370*, *Δrv3005c*). SodA mutants of *Mtb* are not viable, so an *Msm* mutant lacking the orthologous gene was generated (*ΔMsmeg_6427*). The physical interaction of DoxX, SseA, and SodA in the different mutant backgrounds was confirmed by alternatively tagging either with SNAP or

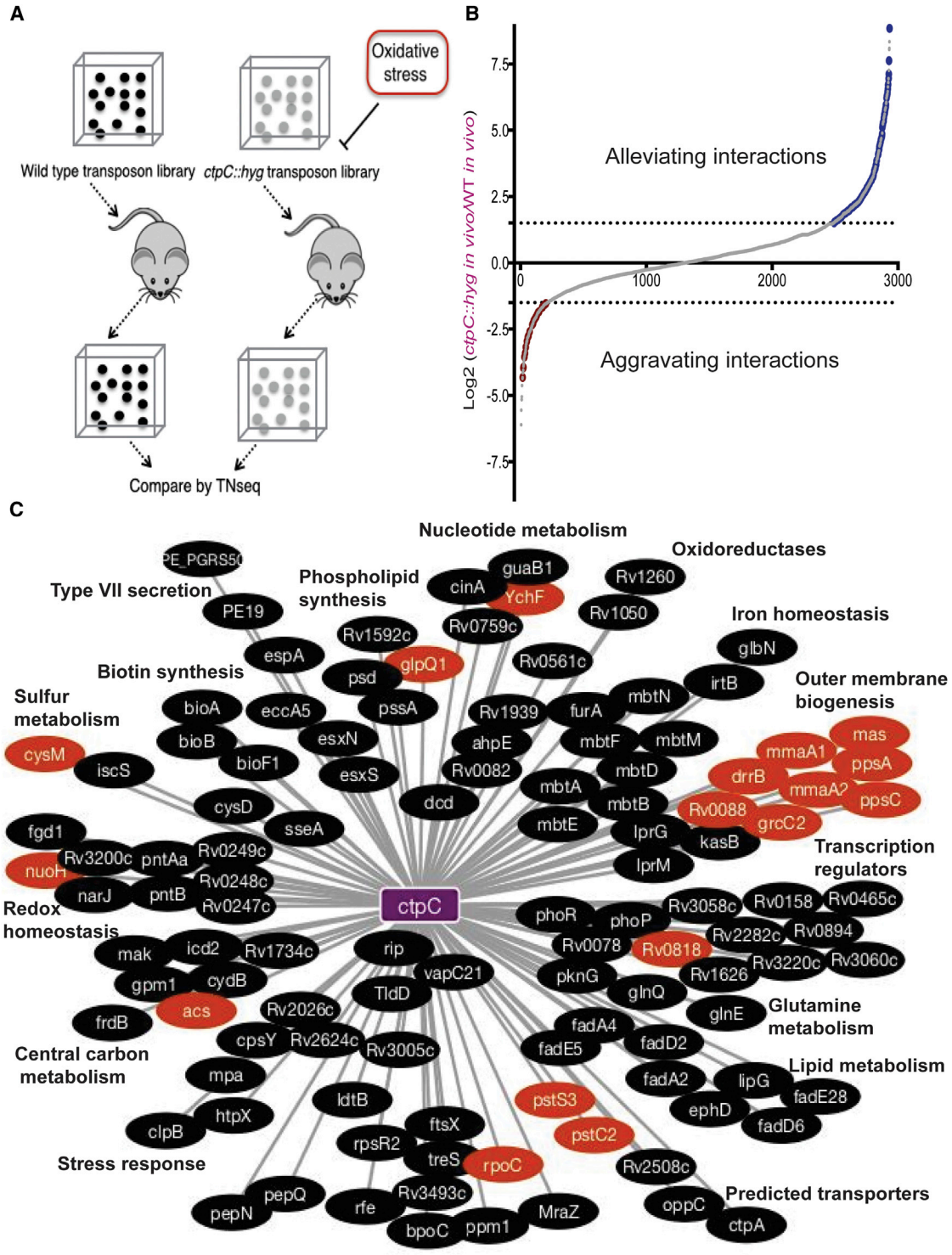

Figure 1. Genetic Screen to Define Oxidative Stress Network

(A) Scheme for identifying genes that are involved in oxidative stress defense during infection. Saturated transposon libraries were generated in WT or *ctpC::hyg* strains, and the respective libraries were used to infect mice. The relative fitness of each mutant was estimated by TnSeq.

(B) The aggravating and alleviating interactions identified by TnSeq analysis described in (A). Genes that are similarly required for in vivo growth in both genetic backgrounds will produce ratios near 1. Alleviating or aggravating transposon insertions will produce numerically larger or smaller ratios in the mutant background, respectively. Dotted lines indicate significance thresholds ($p < 0.05$).

(C) Network map of mutants with predictable functions. Shorter edge lengths indicate stronger interactions. Genes of related functions are grouped in clusters. Red indicates aggravating interactions, and black indicates alleviating interactions, throughout the figure.

A

Mtb protein names	Gene ID	Spectral counts	Peptides Identified
Superoxide dismutase Fe SodA	gi|15610982	41	(K) EDHSAILLNE**K** (N) (R) YAAATSQT**K** (G)
Thiosulfate sulfurtransferase SseA	gi|15610419	6	(R) LVTADWLSAHMGAPGLAIV ESDEDVLLYDVGHIPGAV**K** (I) (R) DYINGEQFAELMD**R** (K) (R) SSHTWFVLTHLLG**K** (A) (R) NYDGSWTEWGNAV**R** (V)
Iron dependent peroxidase Rv0799c	gi|15607939	23	(R) LFAGPRPTELHPFVELTGP**R** (H) (R) HTAPATPGDLLFHI**R** (A) (R) DLLGFVDGTENPSGPIAI**K** (A)
Sulfate-binding lipoprotein (subI)	gi|15609537	5	(K) GIPFGSVVTFVV**R** (A)
Sulfate adenylyltransferase subunit-2 (CysD)	gi|15608425	13	(R) EVAAEFERPVLLFSGG**K** (D) (R) LVVASVQDDIDAG**R** (V) (R) DEFGQWDP**K** (A)

B

Msmeg protein names	Gene ID	Spectral counts	Peptides Identified
Superoxide dismutase Fe SodA	gi|399990630	26	(R) FAAATS**K** (T) (K) GVNDAIA**K** (L)
Thiosulfate sulfurtransferase SseA	gi|399986182	19	(R) QSSGYPVVE**R** (N) (R) VPVAVGPDPGSA**P** (-)

C

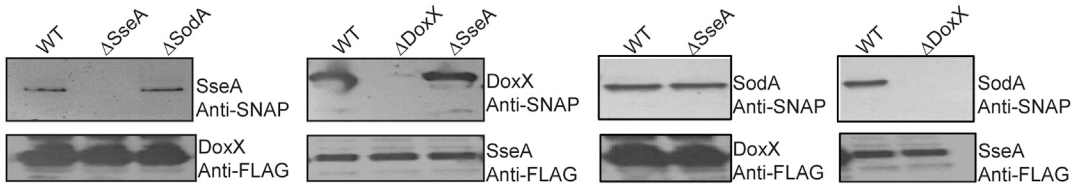

D

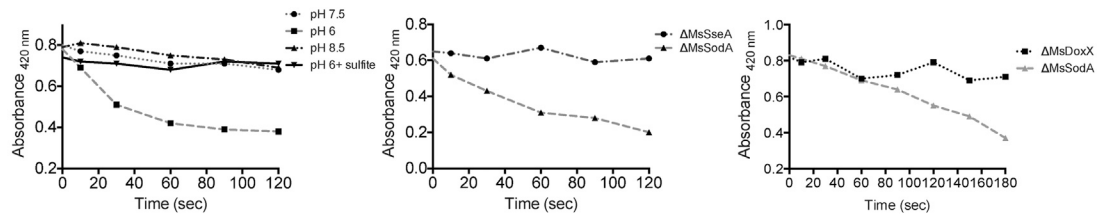

Figure 2. DoxX, SseA, and SodA Form an Oxidoreductase Complex

(A) FLAG-tagged DoxX was purified from detergent extracts of *Mtb*, and interacting proteins were identified by MS/MS.

(B) A similar analysis was performed as (A), but from *Msm* expressing FLAG-DoxX.

(C) Recombinant FLAG-tagged DoxX or SseA were expressed in the indicated strain background, and SNAP-tagged DoxX, SseA, or SodA were simultaneously expressed. FLAG-tagged proteins were purified, and western blot analysis was performed using anti-tag antibody.

(D) Kinetics of DoxX and SseA enzyme activity using potassium ferricyanide as the electron acceptor and measuring absorbance at 420 nm. Enzyme complexes were affinity purified using FLAG-DoxX expressed in WT *Msm*, and the enzyme assay was carried out at different pH values in the presence or absence of sulfite (left). Enzyme complexes were purified using FLAG-DoxX from the indicated mutant strains, and activity was determined at pH 6 (middle). Enzyme complexes were purified using FLAG-SseA from the indicated mutant strains, and kinetics was determined at pH 6 (right). All samples were normalized by relative protein content. Data are representative of three independent experiments.

FLAG tags. DoxX interacts with SseA even in the absence of SodA. However, the interaction of SseA with SodA was dependent on DoxX, indicating that the latter protein nucleated the complex (Figure 2C). The native enzyme complex was purified from WT or mutant strains lacking each gene using either FLAG-tagged DoxX or FLAG-tagged SseA. The complex purified from WT cells possessed thiosulfate oxidation activity (Figure 2D). This reaction was inhibited by sulfite, similar to the inhibition observed for cyanide detoxification by other SseA homologs. Thiosulfate oxidation activity required both DoxX and SseA to be present in the complex, whereas SodA was dispensable (Figure 2D). Thus, DoxX is necessary for SseA activity, and these proteins form a membrane oxidoreductase complex (MRC) that is physically coupled to SodA.

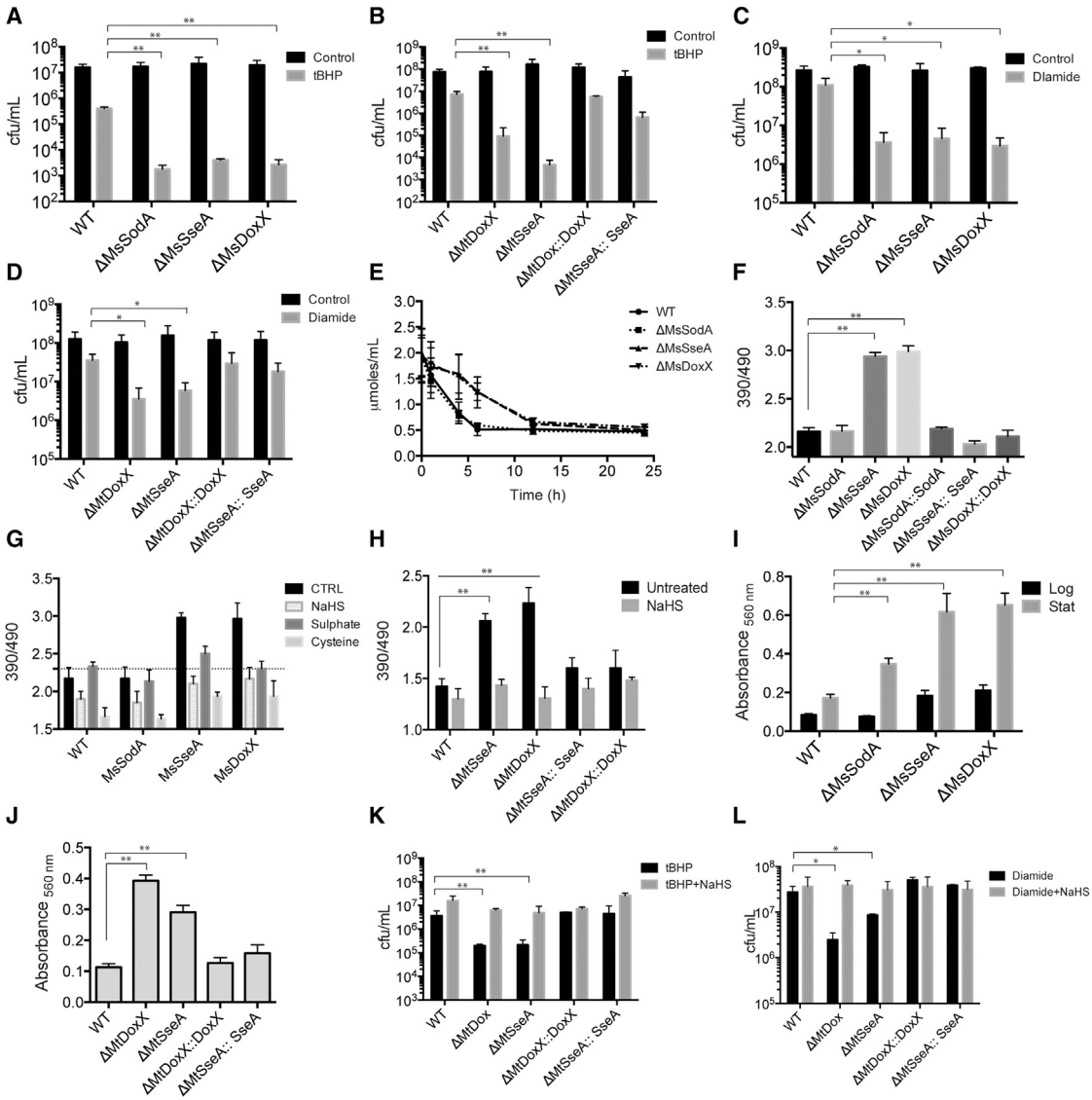

Figure 3. Sensitivity of *sodA*, *sseA*, *and doxX* Mutant Strains to Redox Stressors

Effect of tBHP on viability of *Msm* WT and mutant strains (A) and *Mtb* WT and mutant strains (B). Log phase cultures of the indicated strains were exposed to 1 mM tBHP for 1 hr, and CFU were enumerated. Values represent the mean ± SE of duplicate determinations of experiments repeated thrice. **$p < 0.01$ by unpaired Student's t test. The effect of diamide on *Msm* WT and mutant strains (C) and *Mtb* WT and mutant strains (D) was determined. CFUs were measured after 12 hr of treatment with 5 mM diamide. Values represent the mean ± SE of duplicate determinations of experiments repeated thrice. *$p < 0.05$ by unpaired Student's t test. (E) Conversion of diamide to hydrazine was measured spectrophotometrically at 390 nM at the indicated time points. Values represent the mean ± SE (error bars) of three independent experiments. The rates of diamide conversion for *Msm* WT and *ΔMsSodA* were 0.24 ± 0.08 and 0.21 ± 0.07 µmol/ml/hr, respectively, and *ΔMsDoxX* and *ΔMsSseA* were 0.10 ± 0.05 and 0.10 ± 0.04 µmol/ml/hr, respectively. Ratiometric sensor response of Mrx1-roGFP2 was measured from the indicated *Msm* strains (F) and *Mtb* strains (H) by determining the fluorescence emission at 510 nm after excitation at 390 nm and 490 nm, which indicate the relative abundance of the oxidized and reduced roGFP, respectively. Data are representative of three independent experiments. **$p < 0.01$ by unpaired Student's t test. (G) The redox state of the mycothiol pool was assessed during oxidative stress using the Mrx1-roGFP2 sensor. The indicated strains were exposed to 100 µM of cysteine, sodium sulfate, or NaHS for 1 hr, and the ratiometric sensor response was measured. Lipid hydroperoxides were measured after incubation with FOX2 reagent in *Msm* WT and mutant strains (I) and *Mtb* WT and mutant strains (J). Data are normalized relative to the cell mass. "Log" and "Stat" represent exponential and stationary phases of growth. Data represent the mean of three independent replicates ± SE (error bars). **$p < 0.01$ by unpaired Student's t test. The effect of pretreatment with 100 µM NaHS for 1 hr on tBHP (K) and diamide (L) sensitivity of *Mtb* WT and mutant strains was determined. CFUs were enumerated. Values shown represent the mean ± SE of duplicate determinations of experiments repeated twice. **$p < 0.01$ and *$p < 0.05$ by unpaired Student's t test.

The Coordinated Activities of MRC Components Relieve Oxidative Stress by Maintaining Thiol Homeostasis

To investigate the interdependency between SseA, DoxX, and SodA in the intact cell, we quantified the sensitivity of each mutant strain to oxidative stressors. Consistent with the apparent biochemical dependency between SseA and DoxX, mutation of these genes in *Mtb* (Figures 3B, S2B, and S2D) or *Msm* (Figures 3A, S2C, and S2E) increased sensitivity to

tert-butyl-hydroperoxide (tBHP), cumene hydroperoxide (CHP), and the nitric oxide donor, DETA-NO. In contrast, only the *ΔMsSodA* mutant, and neither the *ΔMsSseA* nor the *ΔMsDoxX* mutant, was sensitive to the superoxide generators, plumbagin and menadione (Figure S2A). Hydrogen peroxide and xanthine oxidase-generated superoxide were not toxic to either WT or mutant strains at the concentrations tested (Figure S2).

Unlike the superoxide generated by plumbagin and menadione, tBHP and CHP react with cytosolic thiols (Fernandes et al., 2010; Kučera et al., 2014). The specific sensitization of *ΔsseA* and *ΔdoxX* strains to tBHP and CHP could reflect a role for the encoded proteins in cytosolic thiol recycling. Consistent with this hypothesis, we observed that mutation of *ΔsseA* and *ΔdoxX* in either *Mtb* or *Msm* increased sensitivity to the thiol-specific oxidant, diamide (Figures 3C and 3D). To estimate the rate of thiol recycling in each mutant, we quantified the rate of diamide reduction to colorless hydrazine, which occurs as a consequence of thiol oxidation. Diamide reduction was significantly retarded in *ΔDoxX* and *ΔSseA* mutants, relative to WT (Figures 3E and S2J), indicating that thiol recycling was impaired. While the *MsSodA* mutant was equally sensitive to diamide as mutants lacking SseA or DoxX, diamide reduction was unimpaired. These results suggest that SseA and DoxX act as a complex to promote resistance to agents that disrupt thiol homeostasis. SodA does not directly influence thiol recycling; however, the unanticipated requirement of SodA for resisting thiol-specific oxidation indicates that this protein plays an essential role in thiol homeostasis as a component of the MRC.

The most abundant small-molecular-weight thiol in mycobacteria is mycothiol (MSH). To determine if MRC influences MSH cycling, we used the Mrx1-roGFP reporter protein to assess the ratio of reduced:oxidized mycothiol (MSH:MSSM) (Bhaskar et al., 2014). In *ΔMsSseA* and *ΔMsDoxX* mutant strains, we found that the MSH:MSSM ratio was significantly lower than WT and *ΔMsSodA* strains (Figure 3F). A similar decrease in MSH:MSSM ratio was observed in the mutant *Mtb* strains, *ΔMtSseA* and *ΔMtDoxX* (Figure 3H), directly implicating the MRC in MSH recycling. The relative oxidation of the MSH/MSSH pool in the *Mtb* mutants was further confirmed by mass spectrometry (Figure S3).

The defect in thiol homeostasis expressed by MRC mutants under unperturbed axenic culture conditions suggested that ROS produced endogenously via respiration might be inefficiently detoxified in these bacteria. Indeed, we found that a stable product of cellular oxidation, lipid hydroperoxides, accumulated in *ΔMsSseA*, *ΔMsDoxX*, *ΔMtSseA*, and *ΔMtDoxX* bacteria compared to WT controls (Figures 3I and 3J). The degree of lipid peroxidation observed in these mutants was significantly greater than even the *ΔMsSodA* mutant. This observation likely explains the presence of phospholipid synthetic genes in the oxidative stress network (Figure 1C). As these cultures contained catalase to reduce exogenous ROS, these data indicate that the MRC plays a significant role in detoxifying endogenously produced radicals.

We used a chemical complementation strategy to investigate whether the observed MSH homeostasis defect of MRC mutants was related to their oxidative stress sensitivity. We found that supplementation with 100 μM sulfur, in the form of cysteine, sulfate (SO_4^{2-}), or hydrogen sulfide (H_2S), could restore the MSH:MSSM ratio of *ΔsseA* and *ΔdoxX* mutants to WT levels in vitro (Figures 3G and 3H). The restoration of MSH:MSSH ratio also reversed the sensitivity of these mutants to diamide and tBHP (Figures 3K and 3L), demonstrating functional complementation. The differing redox potentials of the sulfur in these compounds did not alter this activity. In particular, the ability of sulfate, which has a lower reduction potential than MSH, to restore MSH:MSSM ratio indicated that these supplements were not directly reducing MSSM. Instead, sulfur supplementation likely complements the recycling defect by increasing MSH synthesis, as has been shown for glutathione synthesis in *E. coli* (Loewen, 1979).

MRC Maintains Thiol Homeostasis during Infection

Our initial GI screen was performed using a competitive infection of mouse spleen. To confirm the role of the MRC, we assessed the growth dynamics of the *ΔMtDoxX* and *ΔMtSseA* mutants in a variety of infection models. Bone marrow-derived macrophages were used to quantify the ability of these mutants to grow intracellularly. In resting macrophages, all mutants behaved similarly to WT bacteria. However, in macrophages that were prestimulated with interferon gamma (IFNγ), both *ΔMtSseA* and *ΔMtDoxX* mutants were unable to replicate (Figure 4A). As the antimicrobial effect of IFNγ is at least partially mediated by augmenting the production of ROS and RNI (Podinovskaia et al., 2013), the attenuation of these mutants was consistent with their sensitivity to oxidative stress. This intracellular growth defect was also apparent after low-dose aerosol infection of both resistant (C57BL/6) and susceptible (C3HeB/FeJ) mice (Kramnik et al., 2000) with the *ΔMtDoxX* mutant (Figures 4B and 4C). All growth defects were specific to infection conditions, as both *ΔMtDoxX* and *ΔMtSseA* mutants grew at WT rates in vitro (Figures 4E and 4F).

H_2S is an endogenous metabolite of mammals, and is broadly distributed through tissue after administration of its sodium salt (NaHS) (Wagner et al., 2009). We leveraged the ability of this compound to chemically complement the in vitro defects of MRC mutants to test whether similar mechanisms were likely to underlie the attenuation of MRC mutants during infection. The addition of NaHS completely complemented the intracellular growth defects of *ΔMtSseA* and *ΔMtDoxX* mutants in IFNγ-stimulated macrophages (Figure 4A). To extend these findings to the mouse model, NaHS was delivered continually to animals for 6 weeks, beginning at 4 weeks postinfection. As we observed in macrophage infections, NaHS supplementation significantly increased the growth of *ΔMtDoxX* bacteria to near-WT levels (Figure 4D). In both the macrophage and mouse infection models, NaHS supplementation had no discernable effect on the growth or replication of WT *Mtb*, indicating specific complementation of the MRC mutant phenotype. The ability of sulfur supplementation to complement the in vitro MSH redox defect, oxidative stress sensitivity, and growth during infection supports a primary role for the MRC in maintenance of thiol homeostasis in the oxidative environments encountered during infection.

DISCUSSION

This study describes a systematic genetic approach to decipher the functional network responsible for oxidative defense in *Mtb* during infection. The major SOD of *Mtb*, SodA, was found to

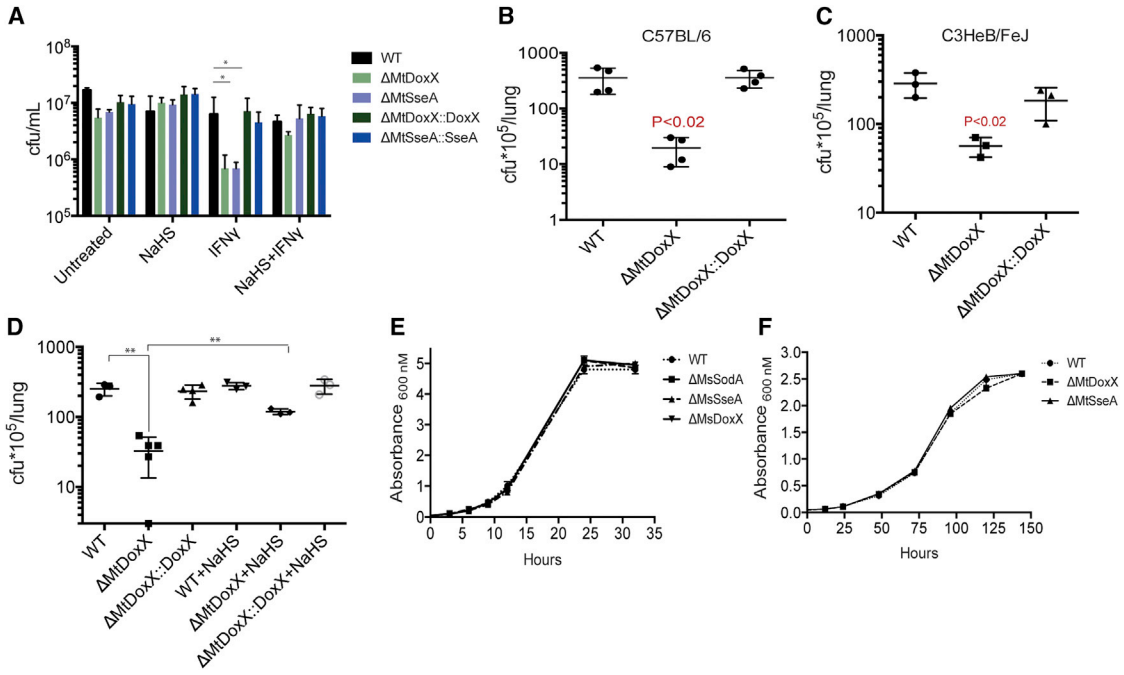

Figure 4. MRC Maintains Thiol Homeostasis In Vitro and during Infection

(A) Immortalized C57BL/6 bone marrow-derived macrophages were infected with *Mtb* mutants in the presence of the indicated compounds. CFU were enumerated at the indicted time points. Groups of C57BL/6 mice (B) or C3HeB/FeJ mice (C) were infected with the indicated *Mtb* strains. Bacterial burdens in the lungs were determined at 4 weeks postinfection. Mice were inoculated with 202 ± 32 CFU of WT, 245 ± 55 CFU of *ΔMtDoxX*, and 173 ± 47 CFU of the complemented mutant (errors indicate SD of duplicate measurements). (D) In vivo chemical complementation. Groups of C57BL/6 mice were infected with the indicated strains. After 4 weeks, mice were administered saline (n = 3) or NaHS (n = 3) for 6 weeks by osmotic minipump. Resulting bacterial burdens in the lungs are shown. Growth measured by optical density (OD_{600}) of *Msm* and mutant strains (E) and *Mtb* and mutant strains (F) grown in 7H9 media.

form a stable complex with two previously uncharacterized proteins, DoxX and SseA, which coordinately act to maintain the redox state of the MSH pool. DoxX and SseA were both required for thiol oxidoreductase activity of the MRC and resistance to specific oxidative stresses that affect the thiol pool. In contrast, SodA was dispensable for thiol recycling, but required for resisting thiol-specific oxidants. These observations imply a biochemical model in which the SseA/DoxX portion of the complex is responsible for recycling thiyl radicals that are formed upon cytosolic thiol oxidation either by peroxides or diamide (Figure S4). This mechanism is analogous to the canonical glutathione (GSH) system, which dissipates free radicals through the formation of a GSH thiyl radical that is recycled through conversion to GSSG by glutaredoxin and then GSH by glutathione reductase (Starke et al., 2003). However, SseA belongs to a large family of ''rhodanese'' enzymes that form a transient sulfane sulfur during catalysis (Toohey, 1989) and thereby use a wide variety of substrates that could include other low-molecular-weight thiols in addition to MSH. In mycobacteria, this promiscuity may be advantageous, as alternative thiol redox buffering systems such as those using ergothionine have been described (Kumar et al., 2011). The requirement for SodA in the MRC is likely due to its ability to detoxify radicals that are known to be generated during the SseA reaction (Remelli et al., 2012). Thus, the physical association between SOD and thiol oxidoreductase activities provides a biochemical explanation for the unexpected diamide sensitivity of SodA-deficient mutants.

While genome-wide GI networks have been described in a number of organisms, these interactions are generally determined under defined in vitro conditions. The plasticity of cellular metabolism implies that the structure of these networks will change in different environments. Indeed, the unanticipated coordination between superoxide detoxification and thiol homeostasis described in this study was discovered because the *Mtb* GI network was defined under relevant environmental conditions that included the complex mixture of host-derived oxidants. These considerations suggest that GI networks are most valuable when they are examined under the correct conditions. In addition to defining functional pathways, GI networks are also useful for identifying genetic synergies that could be exploited therapeutically. Novel treatments that inhibit these synergistic defense mechanisms could be used to accelerate tuberculosis therapy.

EXPERIMENTAL PROCEDURES

Strains and Plasmids Used in the Study

Mtb H37Rv and *Msm* mc^2155 were grown at 37°C in 7H9 and 7H10 media (BD Biosciences) supplemented with 10% OADC enrichment plus hygromycin (50 μg/ml) and kanamycin (25 μg/ml) as needed. *ΔleuD ΔpanCD* auxotrophic *Mtb* was grown in the presence of lysine and pantothenate (Sampson et al., 2004).

Genetic Analysis

Msm and *Mtb* mutants were constructed by allelic exchange, as described previously (Murphy et al., 2015; van Kessel and Hatfull, 2007). Transposon

libraries were made using the pMycoMarT7 transposon in WT and *ctpC::hyg* strains (Sassetti et al., 2001). Colony-forming units (CFU) (10^6) of WT or *ctpC* mutant libraries were introduced intravenously by tail vein injection into four groups of three C57BL/6 mice. At days 0 and 32, the mice were sacrificed, and the surviving bacteria were isolated by plating spleen homogenates. The composition of these libraries was compared by deep sequencing amplicons derived from the transposon-chromosome junctions, as described in the Supplemental Information.

Infection Models

Immortalized C57BL/6 bone marrow-derived macrophages seeded at 1×10^5 cells per well in 24-well plates were infected with *Mtb* at an MOI of 3. Extracellular bacteria were washed away 4 hr later. At day 7, infected macrophages were washed and lysed, and CFUs were enumerated. IFN-γ was added at a concentration of 25 ng/ml. C57BL/6 and C3HeB/FeJ were infected using an aerosol generation chamber (Glas-Col) standardized to deliver ~200 CFU of *Mtb* per mouse. At the indicated time points, animals were sacrificed, and CFU were enumerated from tissue homogenates.

Detailed procedures can be found in the Supplemental Information.

SUPPLEMENTAL INFORMATION

Supplemental Information includes four figures, two tables, and Supplemental Experimental Procedures and can be found with this article online at http://dx.doi.org/10.1016/j.chom.2015.05.008.

AUTHOR CONTRIBUTIONS

S.N., J.E.L., and C.M.S. conceived and designed the experiments. S.N., J.E.L., B.B.M., K.C.M., A.J.O., and H.P.N. performed the experiments. S.N., J.E.L., R.B., H.P.N., S.A.S., and C.M.S. analyzed the data. S.N. and C.M.S. wrote the paper.

ACKNOWLEDGMENTS

We thank J. Lezsyk, K.G. Papavinasasundaram, C. Smith, and X. Meniche for technical assistance; A. Brass, K. Rhee, and M. Volkert for valuable suggestions and reagents; the NIH for awards F32A1093049 (J.E.L.) and U19 AI107774 (C.M.S.); and the Howard Hughes Medical Institute.

Received: November 25, 2014
Revised: April 3, 2015
Accepted: May 13, 2015
Published: June 10, 2015

REFERENCES

Babu, M., Arnold, R., Bundalovic-Torma, C., Gagarinova, A., Wong, K.S., Kumar, A., Stewart, G., Samanfar, B., Aoki, H., Wagih, O., et al. (2014). Quantitative genome-wide genetic interaction screens reveal global epistatic relationships of protein complexes in *Escherichia coli*. PLoS Genet. *10*, e1004120.

Bhaskar, A., Chawla, M., Mehta, M., Parikh, P., Chandra, P., Bhave, D., Kumar, D., Carroll, K.S., and Singh, A. (2014). Reengineering redox sensitive GFP to measure mycothiol redox potential of *Mycobacterium tuberculosis* during infection. PLoS Pathog. *10*, e1003902.

Bryk, R., Lima, C.D., Erdjument-Bromage, H., Tempst, P., and Nathan, C. (2002). Metabolic enzymes of mycobacteria linked to antioxidant defense by a thioredoxin-like protein. Science *295*, 1073–1077.

Chavadi, S.S., Stirrett, K.L., Edupuganti, U.R., Vergnolle, O., Sadhanandan, G., Marchiano, E., Martin, C., Qiu, W.-G., Soll, C.E., and Quadri, L.E.N. (2011). Mutational and phylogenetic analyses of the mycobacterial mbt gene cluster. J. Bacteriol. *193*, 5905–5913.

Cipollone, R., Ascenzi, P., and Visca, P. (2007). Common themes and variations in the rhodanese superfamily. IUBMB Life *59*, 51–59.

Costanzo, M., Baryshnikova, A., Bellay, J., Kim, Y., Spear, E.D., Sevier, C.S., Ding, H., Koh, J.L.Y., Toufighi, K., Mostafavi, S., et al. (2010). The genetic landscape of a cell. Science *327*, 425–431.

Edwards, K.M., Cynamon, M.H., Voladri, R.K., Hager, C.C., DeStefano, M.S., Tham, K.T., Lakey, D.L., Bochan, M.R., and Kernodle, D.S. (2001). Iron-cofactored superoxide dismutase inhibits host responses to *Mycobacterium tuberculosis*. Am. J. Respir. Crit. Care Med. *164*, 2213–2219.

Farhana, A., Kumar, S., Rathore, S.S., Ghosh, P.C., Ehtesham, N.Z., Tyagi, A.K., and Hasnain, S.E. (2008). Mechanistic insights into a novel exporter-importer system of *Mycobacterium tuberculosis* unravel its role in trafficking of iron. PLoS ONE *3*, e2087.

Fernandes, A.S., Gaspar, J., Cabral, M.F., Rueff, J., Castro, M., Batinic-Haberle, I., Costa, J., and Oliveira, N.G. (2010). Protective role of ortho-substituted Mn(III) N-alkylpyridylporphyrins against the oxidative injury induced by tert-butylhydroperoxide. Free Radic. Res. *44*, 430–440.

Garces, A., Atmakuri, K., Chase, M.R., Woodworth, J.S., Krastins, B., Rothchild, A.C., Ramsdell, T.L., Lopez, M.F., Behar, S.M., Sarracino, D.A., and Fortune, S.M. (2010). EspA acts as a critical mediator of ESX1-dependent virulence in *Mycobacterium tuberculosis* by affecting bacterial cell wall integrity. PLoS Pathog. *6*, e1000957.

Griffin, J.E., Gawronski, J.D., Dejesus, M.A., Ioerger, T.R., Akerley, B.J., and Sassetti, C.M. (2011). High-resolution phenotypic profiling defines genes essential for mycobacterial growth and cholesterol catabolism. PLoS Pathog. *7*, e1002251.

Halliwell, B., and Gutteridge, J. (2007). Free Radicals in Biology and Medicine (OUP Oxford).

Hasan, M.R., Rahman, M., Jaques, S., Purwantini, E., and Daniels, L. (2010). Glucose 6-phosphate accumulation in mycobacteria: implications for a novel F420-dependent anti-oxidant defense system. J. Biol. Chem. *285*, 19135–19144.

Jaeger, T., Budde, H., Flohé, L., Menge, U., Singh, M., Trujillo, M., and Radi, R. (2004). Multiple thioredoxin-mediated routes to detoxify hydroperoxides in *Mycobacterium tuberculosis*. Arch. Biochem. Biophys. *423*, 182–191.

Joshi, S.M., Pandey, A.K., Capite, N., Fortune, S.M., Rubin, E.J., and Sassetti, C.M. (2006). Characterization of mycobacterial virulence genes through genetic interaction mapping. Proc. Natl. Acad. Sci. USA *103*, 11760–11765.

Kramnik, I., Dietrich, W.F., Demant, P., and Bloom, B.R. (2000). Genetic control of resistance to experimental infection with virulent *Mycobacterium tuberculosis*. Proc. Natl. Acad. Sci. USA *97*, 8560–8565.

Kučera, O., Endlicher, R., Roušar, T., Lotková, H., Garnol, T., Drahota, Z., and Cervinková, Z. (2014). The effect of tert-butyl hydroperoxide-induced oxidative stress on lean and steatotic rat hepatocytes in vitro. Oxid. Med. Cell. Longev. *2014*, 752506–752512.

Kumar, A., Farhana, A., Guidry, L., Saini, V., Hondalus, M., and Steyn, A.J.C. (2011). Redox homeostasis in mycobacteria: the key to tuberculosis control? Expert Rev. Mol. Med. *13*, e39.

Loewen, P.C. (1979). Levels of glutathione in *Escherichia coli*. Can. J. Biochem. *57*, 107–111.

Müller, F.H., Bandeiras, T.M., Urich, T., Teixeira, M., Gomes, C.M., and Kletzin, A. (2004). Coupling of the pathway of sulphur oxidation to dioxygen reduction: characterization of a novel membrane-bound thiosulphate:quinone oxidoreductase. Mol. Microbiol. *53*, 1147–1160.

Murphy, K.C., Papavinasasundaram, K., and Sassetti, C.M. (2015). Mycobacterial recombineering. Methods Mol. Biol. *1285*, 177–199.

Nandi, D.L., Horowitz, P.M., and Westley, J. (2000). Rhodanese as a thioredoxin oxidase. Int. J. Biochem. Cell Biol. *32*, 465–473.

Newton, G.L., Arnold, K., Price, M.S., Sherrill, C., Delcardayre, S.B., Aharonowitz, Y., Cohen, G., Davies, J., Fahey, R.C., and Davis, C. (1996). Distribution of thiols in microorganisms: mycothiol is a major thiol in most actinomycetes. J. Bacteriol. *178*, 1990–1995.

Padilla-Benavides, T., Long, J.E., Raimunda, D., Sassetti, C.M., and Argüello, J.M. (2013). A novel P(1B)-type Mn2+-transporting ATPase is required for secreted protein metallation in mycobacteria. J. Biol. Chem. *288*, 11334–11347.

Podinovskaia, M., Lee, W., Caldwell, S., and Russell, D.G. (2013). Infection of macrophages with *Mycobacterium tuberculosis* induces global modifications to phagosomal function. Cell. Microbiol. *15*, 843–859.

Remelli, W., Guerrieri, N., Klodmann, J., Papenbrock, J., Pagani, S., and Forlani, F. (2012). Involvement of the *Azotobacter vinelandii* rhodanese-like protein RhdA in the glutathione regeneration pathway. PLoS ONE *7*, e45193.

Sampson, S.L., Dascher, C.C., Sambandamurthy, V.K., Russell, R.G., Jacobs, W.R., Jr., Bloom, B.R., and Hondalus, M.K. (2004). Protection elicited by a double leucine and pantothenate auxotroph of *Mycobacterium tuberculosis* in guinea pigs. Infect. Immun. *72*, 3031–3037.

Sassetti, C.M., and Rubin, E.J. (2003). Genetic requirements for mycobacterial survival during infection. Proc. Natl. Acad. Sci. USA *100*, 12989–12994.

Sassetti, C.M., Boyd, D.H., and Rubin, E.J. (2001). Comprehensive identification of conditionally essential genes in mycobacteria. Proc. Natl. Acad. Sci. USA *98*, 12712–12717.

Singh, A., Crossman, D.K., Mai, D., Guidry, L., Voskuil, M.I., Renfrow, M.B., and Steyn, A.J.C. (2009). *Mycobacterium tuberculosis* WhiB3 maintains redox homeostasis by regulating virulence lipid anabolism to modulate macrophage response. PLoS Pathog. *5*, e1000545.

Starke, D.W., Chock, P.B., and Mieyal, J.J. (2003). Glutathione-thiyl radical scavenging and transferase properties of human glutaredoxin (thioltransferase). Potential role in redox signal transduction. J. Biol. Chem. *278*, 14607–14613.

Toohey, J.I. (1989). Sulphane sulphur in biological systems: a possible regulatory role. Biochem. J. *264*, 625–632.

van Kessel, J.C., and Hatfull, G.F. (2007). Recombineering in *Mycobacterium tuberculosis*. Nat. Methods *4*, 147–152.

Wagner, F., Asfar, P., Calzia, E., Radermacher, P., and Szabó, C. (2009). Bench-to-bedside review: Hydrogen sulfide—the third gaseous transmitter: applications for critical care. Crit. Care *13*, 213.

Wilson, T.M., and Collins, D.M. (1996). ahpC, a gene involved in isoniazid resistance of the *Mycobacterium tuberculosis* complex. Mol. Microbiol. *19*, 1025–1034.

Winterbourn, C.C. (1995). Toxicity of iron and hydrogen peroxide: the Fenton reaction. Toxicol. Lett. *82-83*, 969–974.